

See discussions, stats, and author profiles for this publication at: <https://www.researchgate.net/publication/260716722>

# Inhibition of Ligand Exchange Kinetics via Active-Site Trapping with an Antibody Fragment

ARTICLE in BIOCHEMISTRY · MARCH 2014

Impact Factor: 3.02 · DOI: 10.1021/bi500110j · Source: PubMed

---

READS

42

## 3 AUTHORS:



**David Oyen**

The Scripps Research Institute

5 PUBLICATIONS 17 CITATIONS

SEE PROFILE



**Jan Steyaert**

Vrije Universiteit Brussel

136 PUBLICATIONS 4,719 CITATIONS

SEE PROFILE



**John N Barlow**

GlaxoSmithKline plc.

15 PUBLICATIONS 321 CITATIONS

SEE PROFILE

# Inhibition of Ligand Exchange Kinetics via Active-Site Trapping with an Antibody Fragment

David Oyen,<sup>†,‡,§</sup> Jan Steyaert,<sup>†,‡</sup> and John N. Barlow<sup>\*,†,‡,||</sup>

<sup>†</sup>Structural Biology Brussels, Vrije Universiteit Brussel, Pleinlaan 2, 1050 Brussels, Belgium

<sup>‡</sup>Department of Molecular and Cellular Interactions, Structural Biology Brussels, Vrije Universiteit Brussel, Pleinlaan 2, 1050 Brussels, Belgium

**S** Supporting Information

**ABSTRACT:** We describe the first example of an inhibitory antibody fragment (nanobody ca1697) that binds simultaneously to an enzyme (the enzyme dihydrofolate reductase from *Escherichia coli*) and its bound substrate (folate). Binding of the antibody to the substrate causes a 20-fold reduction in the rate of folate exchange kinetics. This work opens up the prospect of designing new types of antibody-based inhibitors of enzymes and receptors through suitable design of immunogens.

Antibodies make up an important subclass of protein-based modulators, which have been exploited recently for the development of novel and successful therapeutic treatments.<sup>1,2</sup> Despite their importance, our basic understanding of how antibodies can perturb protein structure and function is poor in comparison to our understanding of small molecule modulators of protein function. In part, this is because the experimental testing of inhibition mechanisms is hindered by the large size and complexity of most antibody–antigen systems. We have developed a simple experimental system to investigate antibody modulator mechanisms, consisting of a panel of single-domain antibody fragments (nanobodies)<sup>3</sup> that target the model enzyme dihydrofolate reductase (DHFR) from *Escherichia coli*. DHFR catalyzes the NADPH-dependent reduction of dihydrofolate (H<sub>2</sub>F) to tetrahydrofolate (THF), a key step in thymidine biosynthesis, and as such has been targeted in chemotherapy.<sup>4</sup> DHFR activity can be modulated both allosterically and nonallosterically by nanobodies.<sup>5,6</sup> Here we describe a novel antibody effector mechanism, namely the inhibition of binding of the ligand to and dissociation of the ligand from the DHFR active site as a result of the simultaneous binding of the nanobody to the enzyme and its substrate.

The nanobody ca1697 was identified as a potent inhibitor of DHFR steady-state activity during the screening of a set of nanobodies isolated from two immunized llamas using phage display technology<sup>6</sup> (Figure S1 of the Supporting Information). Surface plasmon resonance analysis indicated that ca1697 binds to apoDHFR tightly [ $K_D = 30$  nM (Figure S2 of the Supporting Information)]. The mechanism of inhibition was examined in greater detail by determining the crystal structure of the DHFR–folate–ca1697 complex at 1.4 Å (the methods of crystallization, data collection, and analysis are described in the Supporting Information, and the crystallographic and refinement statistics

are summarized in Table S1 of the Supporting Information). ca1697 binds head on to the DHFR active site, with the Met20 loop (i.e., active-site loop) adopting the occluded conformation (Figure 1a). This immediately suggests that ca1697 inhibits DHFR activity by constraining Met20 loop movement. Inhibition of Met20 loop movement by an inhibitory nanobody (Nb216) has been described previously.<sup>5</sup> In contrast to Nb216, all three complementary-determining region loops (and no framework residues) of ca1697 interact with DHFR. More than half of the epitope consists of Met20 loop residues, while the other half consists mostly of helix C and the CC loop (Figure 1a). The remainder of the buried surface area consists of two residues of the CD loop.

A unique feature of the ca1697 interaction is that the ca1697 residue R104 hydrogen bonds with the folate tail [i.e., glutamyl carboxylate moiety (Figure 1c)]. The side chain of DHFR residue R52, which ordinarily hydrogen bonds to folate in the absence of a bound nanobody (Protein Data Bank entry 1RX2), makes a new hydrogen bond to ca1697 residue T108. The glutamyl carboxylate moiety of folate is turned toward ca1697 residue R104. Thus, ca1697 perturbs the hydrogen bond pattern between DHFR and folate and forms direct bonding interactions with both DHFR and its substrate.

Stopped-flow fluorescence studies (Figure S3 of the Supporting Information) were undertaken to determine the impact of ca1697 on binding of the substrate H<sub>2</sub>F to apoDHFR ( $k_{on} = 36 \pm 2 \mu\text{M}^{-1} \text{s}^{-1}$ ,  $k_{off} = 39 \pm 10 \text{s}^{-1}$ , and  $K_D = 1.1 \pm 0.3 \mu\text{M}$  for binding of H<sub>2</sub>F to apoDHFR). ca1697 drastically reduces the on rate and the off rate by ~20-fold for H<sub>2</sub>F ( $k_{on} = 1.91 \pm 0.09 \mu\text{M}^{-1} \text{s}^{-1}$ ,  $k_{off} = 1.5 \pm 0.4 \text{s}^{-1}$ , and  $K_D = 0.8 \pm 0.2 \mu\text{M}$  for binding of H<sub>2</sub>F to the DHFR–ca1697 complex).

To examine whether the interactions of R104 with H<sub>2</sub>F played a role in the reduced binding rates, the R104A–ca1697 site-directed mutant was made for crystallization studies (the mutagenesis method is described in the Supporting Information). The crystal structure of the DHFR–folate–R104A–ca1697 complex was determined at 1.9 Å (the methods of crystallization, data collection, and analysis are described in the Supporting Information; the crystallographic and refinement statistics are summarized in Table S1 of the Supporting Information, and the simulated annealing omit  $2|F_o| - |F_c|$  electron density map is shown in Figure S4 of the Supporting

**Received:** January 26, 2014

**Revised:** March 9, 2014

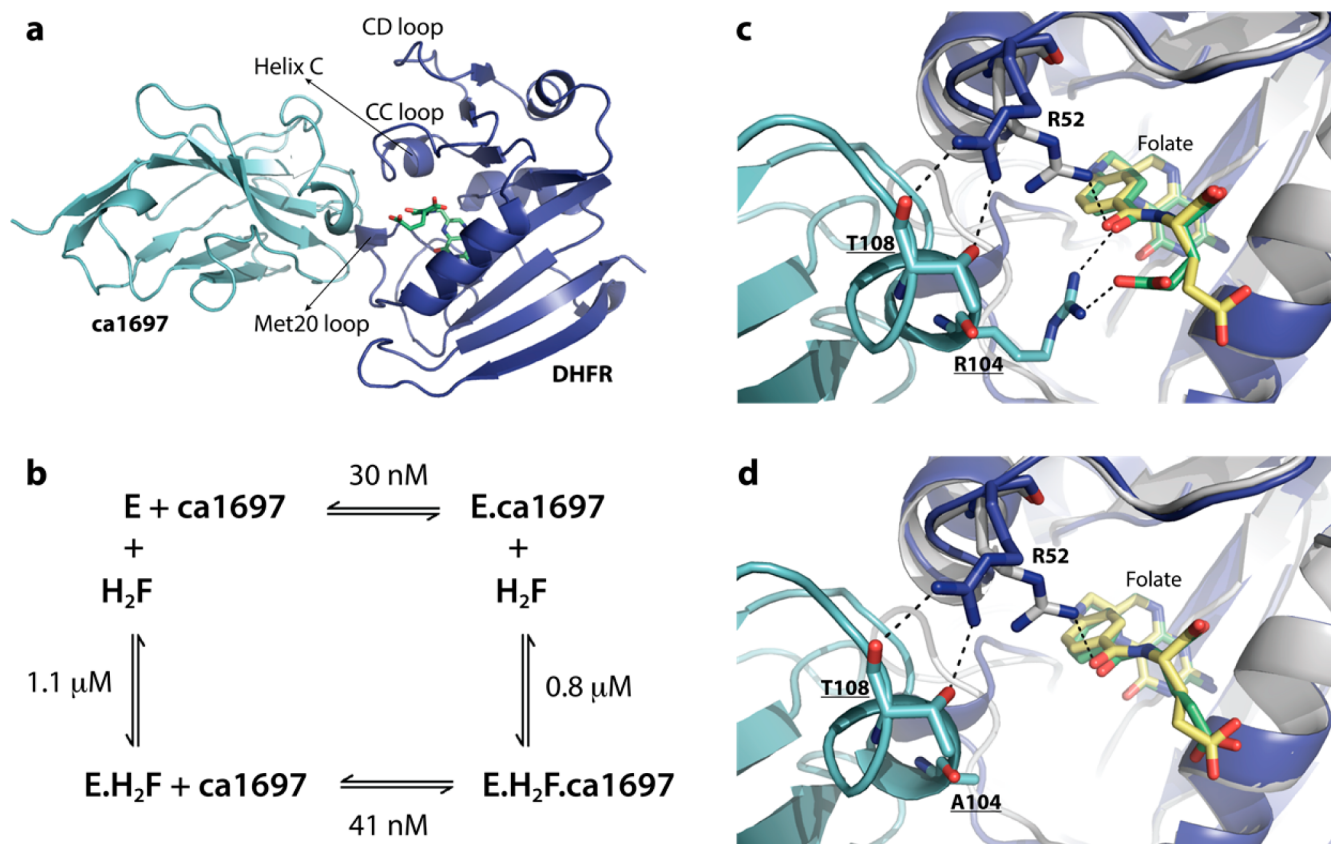


**Figure 1.** DHFR-folate-ca1697 complex structure showing R104 of the ca1697 nanobody as a unique substrate-binding element. (a) ca1697 (cyan) binds the active-site region of DHFR (dark blue). Structural elements that make up the epitope are labeled. The active-site loop (Met20 loop) is in the occluded conformation. (b) Thermodynamic scheme for the dissociation equilibrium constants ( $K_D$ ) for ca1697 and  $H_2F$  with DHFR (E). (c) Detailed view of the interaction with folate. Overlay of the closed DHFR-folate-NADP<sup>+</sup> complex (DHFR colored gray and folate colored yellow) [Protein Data Bank (PDB) entry 1RX2] and the occluded DHFR-folate-ca1697 complex (DHFR colored dark blue, ca1697 colored cyan, and folate colored green). ca1697 residues are underlined. (d) Detailed view of the interaction with folate. Overlay of the closed DHFR-folate-NADP<sup>+</sup> complex (DHFR colored gray and folate colored yellow) (PDB entry 1RX2) and the occluded DHFR-folate-R104A-ca1697 complex (DHFR colored dark blue, R104A-ca1697 colored cyan, and folate colored green). R104A-ca1697 residues are underlined.

Information). The structure reveals that the R104A mutation does not change the overall ca1697 fold or influence the other interactions between ca1697 and DHFR (Figure 1d). Loss of the R104–folate interactions is accompanied by a rotation of the glutamyl carboxylate moiety of folate away from the space previously occupied by the R104 side chain. In addition, an increase in folate electron density is observed, possibly indicating more ordered folate binding. Strikingly, stopped-flow fluorescence studies showed that the rate constant for dissociation of  $H_2F$  from the DHFR· $H_2F$ ·R104A-ca1697 ternary complex is almost fully restored to that observed in the E· $H_2F$  binary complex, with partial restoration of the association rate constant ( $k_{on} = 8.5 \pm 0.2 \mu M^{-1} s^{-1}$ ,  $k_{off} = 30 \pm 1 s^{-1}$ , and  $K_D = 3.5 \pm 0.1 \mu M$  for binding of  $H_2F$  to the DHFR·R104A-ca1697 complex). This indicates that the slow kinetics of binding of  $H_2F$  to the DHFR-ca1697 complex is caused primarily by the R104–folate interaction.

Did the ca1697–folate interaction play a selective role in the affinity maturation of B-lymphocytes directed against the DHFR-folate complex, or is this binding interaction adventitious in origin? This question can be addressed by examining the effect of ca1697 on dihydrofolate binding affinity. The stopped-flow data indicate that ca1697 does not alter dihydrofolate binding affinity: the dissociation constants for dihydrofolate binding with or without ca1697 are the same

within experimental error ( $K_D$  values of  $0.8 \pm 0.2 \mu M$  for binding of  $H_2F$  to the DHFR-ca1697 complex and  $1.1 \pm 0.3 \mu M$  for binding of  $H_2F$  to apoDHFR). Conversely, we can conclude from thermodynamic considerations that folate binding-site occupancy does not alter ca1697 binding affinity (Figure 1b). This suggests, therefore, that the ca1697–folate binding interaction is adventitious in origin.

To the best of our knowledge, ca1697 is the first example of an inhibitory antibody fragment that binds an enzyme and its substrate at the same time. This opens up the exciting possibility of modulating enzyme or receptor activity using therapeutic antibodies that recognize epitopes that incorporate bound substrate or product. Inhibition of protein function by preventing ligand exchange without binding competition between the antibody and ligand (as observed for ca1697) is attractive because the extent of inhibition is not affected by changes in ligand concentration that result from inhibition of protein function. In other cases, antibodies could also show high specificity for the ligand-bound form. Such antibodies could be raised using immunogens that contain tight binding or covalently bound inhibitors. Indeed, this approach has been used to generate antibodies that recognize specific conformational states of proteins (e.g., G protein-coupled receptors).<sup>7</sup>

## ■ ASSOCIATED CONTENT

### 📄 Supporting Information

Details of the materials and methods, surface plasmon resonance profiles, stopped-flow data, simulated annealing omit maps, and crystallographic and refinement statistics. This material is available free of charge via the Internet at <http://pubs.acs.org>.

### Accession Codes

Coordinates have been deposited in the Protein Data Bank as entries 4I13 and 4I1N for the DHFR-folate-ca1697 complex and the DHFR-folate-R104A-ca1697 complex, respectively.

## ■ AUTHOR INFORMATION

### Corresponding Author

\*E-mail: [john.n.barlow@gsk.com](mailto:john.n.barlow@gsk.com). Phone: +32 (0)2 656 5651.

### Present Addresses

<sup>§</sup>D.O.: Department of Molecular Biology, The Scripps Research Institute, MB2, 10550 N. Torrey Pines Rd., La Jolla, CA 92037.

<sup>||</sup>J.N.B.: GSK Vaccines, Rue de l'institut 89, 1330 Rixensart, Belgium.

### Author Contributions

D.O. and J.N.B. designed the experiments. D.O. performed the experiments. J.N.B. and J.S. cosupervised the project, and all authors prepared the manuscript.

### Funding

This study was supported by grants from the Research Foundation-Flanders and the Flemish Institute for Biotechnology.

### Notes

The authors declare no competing financial interest.

## ■ ACKNOWLEDGMENTS

We thank Nele Buys, Katleen Willibal, and Els Pardon for technical advice.

## ■ REFERENCES

- (1) Beck, A., Wurch, T., Bailly, C., and Corvaia, N. (2010) *Nat. Rev. Immunol.* 10, 345–352.
- (2) Leader, B., Baca, Q. J., and Golan, D. E. (2008) *Nat. Rev. Drug Discovery* 7, 21–39.
- (3) Muyldermans, S. (2013) *Annu. Rev. Biochem.* 82, 775–797.
- (4) Schnell, J. R., Dyson, H. J., and Wright, P. E. (2004) *Annu. Rev. Biophys. Biomol. Struct.* 33, 119–140.
- (5) Oyen, D., Srinivasan, V., Steyaert, J., and Barlow, J. N. (2010) *J. Mol. Biol.* 407, 138–148.
- (6) Oyen, D., Wechselberger, R., Srinivasan, V., Steyaert, J., and Barlow, J. N. (2013) *Biochim. Biophys. Acta* 1834, 2147–2157.
- (7) Rasmussen, S. G. F., Choi, H. J., Fung, J. J., Pardon, E., Casarosa, P., Chae, P. S., DeVree, B. T., Rosenbaum, D. M., Thian, F. S., Kobilka, T. S., Schanpp, A., Konetzki, I., Sunahara, R. K., Gellman, S. H., Pautsch, A., Steyaert, J., Weis, W. I., and Kobilka, B. K. (2010) *Nature* 469, 175–180.